Jurnal Penelitian Fisika dan Aplikasinya (JPFA)
Volume 15, Issue 1, 52-70 2025
https://journal.unesa.ac.id/index.php/jpfa/
p-ISSN: 2087-9946
e-ISSN: 2477-1775

Primordial Helium In The Left-Right Symmetry Model With Extra Scalar Fields

Istikomah [1,a,*], Amara Ega Prasheylia [1,b] , Hamdan Hadi Kusuma [1,c]

[1] Physics Department, Universitas Islam Negeri Walisongo, Semarang 50185, Indonesia

e-mail: [a*] istikomah@walisongo.ac.id , [b] amaraega@gmail.com , [c] hamdanhk@walisongo.ac.id
* Corresponding Author

Received: 28 December 2024 ; Revised: 10 June 2025 ; Accepted: 2 June 2025

Abstract

Big Bang Nucleosynthesis (BBN) is a crucial phase in the universe's evolution, occurring approximately 1 second after the Big Bang. The BBN theory predicts a primordial Helium-4 abundance of about 25%, offering key limits on the number of light particles present at BBN temperatures. The Left-Right Symmetry Model with an Extra Scalar Field is a development of the Standard Model that adds a massive scalar field, which can decay into relativistic particles. This research aims to determine the temperature ratio between the right and left sectors, the mass limit of the massive scalar field consistent with BBN constraints, and the primordial helium abundance. This research is theoretical. The research objectives can be achieved with various methods; the Yukawa Lagrangian and the Scalar Potential are depicted in a Feynman Diagram, which then calculates each sector's decay rate and temperature changes. The temperature ratio of the right and left sectors when the BBN took place in this model was 0.08-0.09. The BBN constraint imposes a dimensionless bound expressed as the mass ratio of the scalar field in the right sector to that in the left sector is $m_{\chi_R}/m_{\chi_L} \approx 0.09 - 0.10$. *The abundance of primordial Helium-4 in the left sector is 25%, according to the Standard Model, while primordial Helium-4 in the right industry is 79%-87%. Thus, the Left-Right Symmetry Model with Extra Scalar mode satisfies the constraints of BBN words.*

Keywords: *Primordial Helium; Standard Model; Big Bang Nucleosynthesis (BBN); Left-Right Symmetry; Feynman Diagram*

How to cite: Istikomah, Prasheylia AE, Kusuma HH. Primordial Helium In The Left-Right Symmetry Model With Extra Scalar Fields. *Jurnal Penelitian Fisika dan Aplikasinya (JPFA)*. 2025; 15(1): 52-70. DOI: https://doi.org/10.26740/jpfa.v15n1.p52-70.

INTRODUCTION

Big Bang Nucleosynthesis (BBN), proposed by George Gamow in 1946, is a crucial phase in the evolution of the universe, approximately one second after the Big Bang [1]. Both the Standard Model of Cosmology and Particle Physics can describe cosmological phenomena from the moment of the Big Bang to the era of Big Bang Nucleosynthesis. The Standard Model allows us to extrapolate the state of the universe into the past up to $t \sim 10^{-12}\ s$. [2]. In the time interval, $10^{-12} - 10^{-2} s$ The universe experienced an electroweak transition and a strong-interaction transition. At a $10^{-1} s$ At a time interval, the neutrinos escape from thermal equilibrium, a process called neutrino decoupling. Next, we enter the BBN period, which occurs after one second. [3].

BBN formed primordial light nuclei when the universe's temperature was around 1 MeV to

several KeV. [3]. During the BBN era, protons and neutrons will combine to form light nuclei, such as primordial helium-4. This BBN theory predicts a primordial Helium-4 abundance of around 25%. This prediction limits the number of light particles at the BBN temperature. For example, according to the Standard Model, there are three types of neutrinos. However, if additional types of light neutrinos exist, the temperature must be lower than the photon temperature at the time of BBN. [1]. The additional light neutrinos allowed by BBN are around $\triangle N_{\nu} < 0,2 - 0,3$, so this prediction imposes a constraint on all extensions of the Standard Model. [4].

The Standard Model needs expansion because it has several weaknesses. Its weaknesses are that it cannot explain hierarchy problems and dark matter. [5]. The other mysteries that cannot be explained are the matter-antimatter asymmetry and neutrino oscillations. [6]. So, we need to construct Expansions of the Standard Model. There are some extensions of the Standard Model, such as the Minimal Extension, which introduces a new scalar particle with its own mass generation mechanism; however, its cosmological effects have not yet been studied. [7,8]. The Grand Unified Theory with discrete flavor symmetry, such as S_4, has successfully explained the fermion mass structure and mixing. However, the cosmological implications of additional scalar fields in the model, particularly for Big Bang Nucleosynthesis and the abundance of light elements, have not been thoroughly studied. [9]. The SU(5)-based Grand Unified Theory model with modular A_4 symmetry has successfully provided a highly predictive description of fermion masses and mixings, particularly in the neutrino sector, including predictions for the maximum mixing angle and leptonic CP violation. However, these studies are generally limited to the flavor sector and low-energy phenomenology, without discussing the cosmological implications of the additional fields introduced. In particular, the impact of the scalar sector, flavors, and new particles on the evolution of the early universe, such as Big Bang Nucleosynthesis and the abundance of light elements, has not been studied. Therefore, a research gap remains, as the consistency of GUT models with additional scalar charges needs to be tested against the constraints of early cosmology. [10].

The mirror model developed by Mohapatra and Nasri [11]. Complies with BBN constraints by assuming the post-inflation reheating temperature in the mirror sector is supposed to be lower by about a factor of 10 than in the visible sector to keep the mirror sector from being in thermal contact with the standard industry. The model with mirror symmetry studied by Satriawan [12]. Also, it avoided the BBN problem by assuming the real-sector temperature was higher than the mirror-sector temperature. Kawasaki et al. [13] examined the effects of massive particle decay, which did not affect the abundance of ancient Helium-4 with a lifetime limit of around $10^{-2} s$. Boyarsky et al. [14] investigated a model involving the decay of massive neutral leptons, demonstrating that the BBN constraints could be satisfied if the particle's lifetime were less than 0.02 seconds.

J. C. Pati Salam [15] was the first to introduce the Left-Right Symmetry Model (LRS Model). Left-handed and right-handed particles are treated the same in this model. One aim of developing this model is to explain parity-symmetry violations and charge conjugation. Parity violation, usually observed at low energies, will be followed when symmetry breaking occurs at high energies. Right-handed neutrinos are an automatic consequence of the LRS Model so that this model can explain the small mass of neutrinos through the see-saw mechanism. During its development, the Left-Right Symmetry Model also introduced additional bidoublet scalars in its scalar sector. [16–19]. Apart from that, some developments do not introduce bidoublet scalars but only introduce additional doublet and singlet scalars in the scalar sector. [20–22].

Recent developments in the LRS Model, such as the Minimal LRS Model and the New LRS

Model, ensure BBN constraints are met by stabilizing massive neutrinos or by adjusting the temperature ratios between different sectors. [19,21]. The Modified LRS Model integrates Higgs and t- and tau-boson mass formulations consistent with the Standard Model while addressing dark matter and neutrino mass issues. [20,23–24].

Despite various extensions to the Standard Model—such as the minimal extension, Grand Unification theory, mirror models, and Left-Right Symmetry (LRS)—most studies remain focused on particle phenomenology and fermion mass generation, with limited attention to the cosmological constraints of the early universe. In particular, the embedding of scalar fields and additional particles has not been thoroughly analyzed with respect to BBN constraints, especially those related to primordial helium-4. Existing approaches often rely on a temperature hierarchy between sectors or adjustments to particle lifetimes to meet the BBN constraints, without explicitly tracking the thermal evolution of the two industries from post-inflationary reheating to the BBN epoch.

In this research, we develop a Left-Right Symmetry model with an additional scalar field, in which parity at the beginning of the Big Bang is symmetric and subsequently undergoes spontaneous breaking, resulting in two sectors—a left-hand sector and a right-hand sector—existing in the same universe but with different thermal properties. This difference in temperature evolution allows each sector to undergo separate Big Bang nucleosynthesis (BBN). This approach is phenomenologically hybrid: unlike mirror models that separate the real and mirror sectors into distinct universes, this model maintains a single universe with two post-parity-breaking sectors. Therefore, this study aims to analyze the temperature evolution in both sectors from post-inflationary reheating to the BBN process. The light particles introduced in this model could influence the discussion of primordial helium-4, necessitating further research on the constraints of BBN in the context of models that address them. It is important to understand when BBN occurred and to disentangle primordial helium in both sectors.

METHOD

This research is theoretical. Particle interactions are identified by examining the Higgs potential and the Yukawa Lagrangian, illustrated using Feynman diagrams. Subsequently, the interaction probability is calculated by applying the Feynman rules within the Toy Theory framework. [25]. The decay rate, on the other hand, is determined using the Golden Rule. Temperature evolution can be known by finding the ratio of the initial and final temperatures caused by the decay of massive particles, which is given by Equation (1) [26].

$$\left(\frac{S_f}{S_i}\right)^{4/3} \cong \left(\frac{T_f}{T_i}\right)^4 \cong \frac{2,42 g_{*I}^{\frac{1}{3}}}{s_k^{\frac{4}{3}} m_{pl}^{\frac{2}{3}}} \left[\sum_k \left(m_k Y_{ki}\right)^{\frac{4}{3}} \left(\sum_n \Gamma_n\right)_n^{-\frac{2}{3}}\right] \quad (1)$$

Where $Y_{ki} = \frac{n_i}{s}$. The number density of particle species is determined by equation (2) [3].

$$n_i = g_i \left(\frac{m_i T}{2\pi}\right)^{\frac{3}{2}} e^{\frac{\mu_i - m_i}{T}} \quad (2)$$

The neutrons and protons that have survived since the beginning of BBN combine to form the primordial helium-4 nucleus. The primordial helium abundance in the mirror sector can be calculated using the formula in Equation (3) [27–28].

$$Y_{4R} \cong \frac{2\exp\left[-t_N \Big/ \tau_n \left(1+\left(T_R/T_L\right)^{-4}\right)^{\frac{1}{2}}\right]}{1+\exp\left[\Delta m \Big/ T_W \left(1+\left(T_R/T_L\right)^{-4}\right)^{\frac{1}{6}}\right]} \tag{3}$$

These equations enable the precise determination of the primordial Helium-4 abundance.

Calculation Procedure

The quantitative results in this study were obtained without performing numerical simulations. Instead, we employ an analytical approach to estimate orders. Equation (1) is used to estimate the temperature ratio between the right and left sectors. This equation encompasses numerous interactions involving massive particle decays and their corresponding decay rates. The approximation is performed by retaining only the dominant decay. Equation (2) is used to estimate the particle number density, which, in turn, affects the temperature ratio. The approximation is carried out by keeping only the leading mass order. Equation (3) is used to estimate the helium content in the right sector and is an estimate of the ratio between the known sectors. The neutron lifetime in the right sector is τ_n~886 s. The symbol t_N~200 s represents the age of the universe when deuterium freezes. The symbol T_W~0.75 MeV is the temperature at which the neutron-proton freezes out. The symbol $\Delta m = 1.3$ MeV is the difference in the masses of neutrons and protons.

LEFT-RIGHT SYMMETRY MODEL WITH EXTRA SCALAR FIELD

The Left-Right Symmetry Model with an additional scalar field is a variation of the LRS Model that incorporates a new scalar field. This model is constructed to be invariant under the gauge group. $SU(3)_C \otimes SU(2)_L \otimes SU(2)_R \otimes U(1)_{B-L}$. The proposed particles are divided into two sectors, namely the left and right sectors, as shown in Table 1. In this model, each Left-handed (L) field in the left sector has a Right-handed (R) field pair in the right sector; this also applies to gauge bosons that correspond to each other, allowing the definition of parity symmetry in the sense of Equation (4). The fermion particles in the left sector are Standard Model particles with the addition of the right-handed neutrino ν_R. The parity transform can change the left-handed and right-handed fields through transformations, as shown by Equation (4).

$$P: \psi_L \rightarrow \gamma_0 \psi_R, \qquad \psi_R \rightarrow \gamma_0 \psi_L \tag{4}$$

The symmetry that applies to this model, according to Table 4.1, is shown by Equation (5).

$$\begin{aligned} q_L &\leftrightarrow Q_R \\ \ell_L &\leftrightarrow L_R \\ u_R &\leftrightarrow U_L \end{aligned} \tag{5}$$

The fermions in the right sector are duplicates of the left-sector fermions, with a similar fundamental representation. The scalar field in this model, shown in Table 1, has the same B-L numbers. B-L is the baryon number and lepton number, respectively; this is because parity symmetry in this model only changes chirality, not B-L.

This model introduces eight new scalar fields—extra additions, as shown in Table 1. The assumption of introducing eight scalar fields in this model is

1. The two primary doublet scalar fields are φ_L and φ_R

When spontaneous symmetry breaking occurs, both primary scalar fields will obtain a Vacuum Expectation Value (VEV). Then it will generate Dirac fermion and boson masses in the left- and right-handed sectors.

2. The two new doublet scalar fields are χ_L and χ_R

   The two new doublet scalar fields are involved in the phenomenological symmetry-breaking process. The scalar fields χ_L and χ_R have the exact fundamental representation as in the doublet fermions q_L and Q_R.

3. The four new singlet scalar fields are η, ξ, ρ and ω

   The four singlet scalar fields act as mediators between the left- and right-handed sectors and may also be viewed as leptoquark particles that facilitate lepton-quark decay.

4. Extra scalar fields do not affect the primordial helium abundance that occurred during the Big Bang Nucleosynthesis (BBN).

Table 1. Fundamental Representative Fermion and Scalar Field Particles

Left Sector					
Fermion	Rep	B-L	Scalar	Rep	B-L
ℓ_L	$(\mathbf{1},\mathbf{2},\mathbf{1},-1)$	-1	φ_L	$(\mathbf{1},\mathbf{2},\mathbf{1},-1)$	-1
ν_R	$(\mathbf{1},\mathbf{1},\mathbf{1},0)$	0	η	$(\mathbf{1},\mathbf{1},\mathbf{1},0)$	0
e_R	$(\mathbf{1},\mathbf{1},\mathbf{1},-1)$	-1	ξ	$(\mathbf{1},\mathbf{1},\mathbf{1},-1)$	-1
q_L	$\left(\mathbf{3},\mathbf{2},\mathbf{1},\frac{1}{3}\right)$	$\frac{1}{3}$	χ_L	$\left(\mathbf{3},\mathbf{2},\mathbf{1},\frac{1}{3}\right)$	$\frac{1}{3}$
u_R	$\left(\mathbf{3},\mathbf{2},\mathbf{1},\frac{1}{3}\right)$	$\frac{1}{3}$	ρ	$\left(\mathbf{3},\mathbf{2},\mathbf{1},\frac{1}{3}\right)$	$\frac{1}{3}$
d_R	$\left(\mathbf{3},\mathbf{2},\mathbf{1},-\frac{1}{3}\right)$	$-\frac{1}{3}$	ω	$\left(\mathbf{3},\mathbf{2},\mathbf{1},-\frac{1}{3}\right)$	$-\frac{1}{3}$
Right Sector					
Fermion	Rep	B-L	Scalar	Rep	B-L
L_R	$(\mathbf{1},\mathbf{1},\mathbf{2},-1)$	-1	φ_R	$(\mathbf{1},\mathbf{1},\mathbf{2},-1)$	-1
N_L	$(\mathbf{1},\mathbf{1},\mathbf{1},0)$	0	η^*	$(\mathbf{1},\mathbf{1},\mathbf{1},0)$	0
E_L	$(\mathbf{1},\mathbf{1},\mathbf{1},-1)$	-1	ξ^*	$(\mathbf{1},\mathbf{1},\mathbf{1},-1)$	-1
Q_R	$\left(\mathbf{3},\mathbf{1},\mathbf{2},\frac{1}{3}\right)$	$\frac{1}{3}$	χ_L	$\left(\mathbf{3},\mathbf{1},\mathbf{2},\frac{1}{3}\right)$	$\frac{1}{3}$
U_L	$\left(\mathbf{3},\mathbf{1},\mathbf{2},\frac{1}{3}\right)$	$\frac{1}{3}$	ρ^*	$\left(\mathbf{3},\mathbf{1},\mathbf{2},\frac{1}{3}\right)$	$\frac{1}{3}$
D_L	$\left(\mathbf{3},\mathbf{1},\mathbf{2},-\frac{1}{3}\right)$	$-\frac{1}{3}$	ω^*	$\left(\mathbf{3},\mathbf{1},\mathbf{2},-\frac{1}{3}\right)$	$-\frac{1}{3}$

There are two symmetry-breaking stages in the gauge group used in the LRS Model with Extra Scalar Fields. In the symmetry-breaking scheme with the assumptions, the first symmetry breaking occurred at universe energies of around 10 TeV. When the scalar field χ_L and the scalar field χ_R take the VEV value equal to zero as shown by equation (6).

$$\langle \chi_L \rangle = 0; \langle \chi_R \rangle = 0 \tag{6}$$

Equation (7) shows that singlet scalar fields such as η, ξ, ρ and ω also get a VEV value of zero,

$$\langle \eta \rangle = \langle \xi \rangle = \langle \rho \rangle = \langle \omega \rangle = 0 \tag{7}$$

The gauge group $SU(3)_C \otimes SU(2)_L \otimes SU(2)_R \otimes U(1)_{B-L}$ breaks down to become the Standard Model gauge group $SU(3)_C \otimes SU(2)_L \otimes U(1)_Y$. The left and right sectors remain symmetrical in terms of temperature and particle number. The photon masses in both sectors are also zero. The second breaking of symmetry occurs when the scalar field. φ_L and the scalar field φ_R take the VEV at a temperature of the universe of about 10^2 GeV. The VEV value is shown in Equation (8).

$$\langle \varphi_L \rangle = \frac{1}{\sqrt{2}} \begin{pmatrix} \upsilon_L \\ 0 \end{pmatrix}; \langle \varphi_R \rangle = \frac{1}{\sqrt{2}} \begin{pmatrix} \upsilon_R \\ 0 \end{pmatrix} \tag{8}$$

Symmetry breaking occurs in the gauge group $SU(3)_C \otimes SU(2)_L \otimes U(1)_Y$ to become the gauge group $SU(3)_C \otimes U(1)_{em}$.

SCALAR POTENTIAL

The scalar field potential represents the interaction among scalar fields, as shown by Equation (9)

$$\begin{aligned} V = & -\mu_L^2 \varphi_L^\dagger \varphi_L - \mu_R^2 \varphi_R^\dagger \varphi_R + \mu_\eta^2 |\eta|^2 + \mu_\xi^2 |\xi|^2 - \mu_{\chi_L}^2 \chi_L^\dagger \chi_L - \mu_{\chi_R}^2 \chi_R^\dagger \chi_R + \mu_\rho^2 |\rho|^2 + \mu_\omega^2 |\omega|^2 \\ & + \lambda_1 \left|\varphi_L^\dagger \varphi_L\right|^2 + \lambda_2 \left|\varphi_R^\dagger \varphi_R\right|^2 + \lambda_3 |\eta|^4 + \lambda_4 |\xi|^4 + \lambda_5 |\chi_L|^4 + \lambda_6 |\chi_R|^4 + \lambda_7 |\rho|^4 + \lambda_8 |\omega|^4 \\ & + \epsilon_1 \left|\varphi_L^\dagger \varphi_L\right| \left|\varphi_R^\dagger \varphi_R\right| + |\eta|^2 \left(\epsilon_2 \varphi_L^\dagger \varphi_L + \epsilon_3 \varphi_R^\dagger \varphi_R\right) + \xi^2 \left(\epsilon_4 \varphi_L^\dagger \varphi_L + \epsilon_5 \varphi_R^\dagger \varphi_R\right) + \epsilon_6 \varphi_L^\dagger \varphi_L \chi_L^\dagger \chi_L \\ & + \epsilon_7 \varphi_L^\dagger \varphi_L \chi_R^\dagger \chi_R + \epsilon_8 \varphi_R^\dagger \varphi_R \chi_L^\dagger \chi_L + \epsilon_9 \varphi_R^\dagger \varphi_R \chi_R^\dagger \chi_R + |\rho|^2 \left(\epsilon_{10} \varphi_L^\dagger \varphi_L + \epsilon_{11} \varphi_R^\dagger \varphi_R\right) \\ & + |\omega|^2 \left(\epsilon_{12} \varphi_L^\dagger \varphi_L + \epsilon_{13} \varphi_R^\dagger \varphi_R\right) + \epsilon_{14} \chi_L^\dagger \chi_L \chi_R^\dagger \chi_R + |\eta|^2 \left(\delta_1 \chi_L^\dagger \chi_L + \delta_2 \chi_R^\dagger \chi_R\right) \\ & + |\xi|^2 \left(\delta_3 \chi_L^\dagger \chi_L + \delta_4 \chi_R^\dagger \chi_R\right) + |\rho|^2 \left(\delta_5 \chi_L^\dagger \chi_L + \delta_6 \chi_R^\dagger \chi_R\right) + |\omega|^2 \left(\delta_7 \chi_L^\dagger \chi_L + \delta_8 \chi_R^\dagger \chi_R\right) \\ & + |\eta| \left(\alpha_1 \varphi_L^\dagger \varphi_L + \alpha_2 \varphi_R^\dagger \varphi_R\right) + \alpha_3 \eta |\xi|^2 + \eta \left(\alpha_4 \chi_L^\dagger \chi_L + \alpha_5 \chi_R^\dagger \chi_R\right) + \alpha_6 \eta \rho^2 + \alpha_7 \eta \omega^2 + \text{h. c.} \end{aligned} \tag{9}$$

The parameters $\mu_L, \mu_R, \mu_\eta, \mu_\xi, \mu_\chi, \mu_\rho,$ and μ_ω were related to terms indicating the mass of the scalar field. The λ_i parameter indicates the self-coupling of interactions. The ϵ_i is a parameter that indicates the coupling between the left-right scalar field sector. The parameter δ_i is a coupling between a heavy and a light scalar. The parameter α_i It is a coupling between three scalar interactions. When spontaneous symmetry breaking occurs, the VEV and mass of each scalar field can be determined as shown in Equations (10a) and (10b).

$$\upsilon_L = \pm \sqrt{\frac{4\mu_L^2 \lambda_1 - 2\delta_1 \mu_R^2}{4\lambda_1 \lambda_2 - \delta_1^2}} \tag{10.a}$$

$$\upsilon_R = \pm \sqrt{\frac{4\mu_R^2 \lambda_2 - 2\delta_1 \mu_L^2}{4\lambda_1 \lambda_2 - \delta_1^2}} \tag{10.b}$$

The VEV value expressions in equations (10.a) and (10.b) for ν_L and ν_R are symmetrical or have the same shape due to left-right symmetry. If the VEV values are not very different, $\upsilon_L \approx \upsilon_R$, then this will cause problems. The mass of the W left-sector gauge boson has been measured experimentally at the LHC. [22]. This result can be used to determine the mass of the W right-sector gauge boson. This problem can be overcome by assuming that the two VEVs differ $\upsilon_L \neq \upsilon_R$. The υ_R value is greater than the value. Based on the research results of Coutinho et al. [29], the lower limit for the VEV can guarantee that the particles' mass in the right sector is greater than that in the left sector. The scalar is the Higgs field in the Standard Model in the left sector, so that the VEV value,

namely υ_L, is the same as the VEV value of the Higgs, 246 GeV. [30].

Generation of scalar-field mass occurs when the VEV expands away from its field value. The mass of the scalar fields in the LRS Model with Extra Scalar Field is shown by Equation (11)-(18).

$$m_{\varphi_L} = \sqrt{\lambda_1 \upsilon_L{}^2} \tag{11}$$

$$m_{\varphi_R} = \sqrt{\lambda_1 \upsilon_R{}^2} \tag{12}$$

$$m_{\eta} = \sqrt{\frac{1}{2}(\grave{o}_2 \upsilon_L^2 + \grave{o}_3 \upsilon_R{}^2) - \mu_{\eta}^2} \tag{13}$$

$$m_{\xi} = \sqrt{\mu_{\xi}^2 + \frac{1}{2}(\grave{o}_2 \upsilon_L^2 + \grave{o}_3 \upsilon_R{}^2)} \tag{14}$$

$$m_{\chi_L} = \sqrt{\frac{1}{2}(\grave{o}_6 \upsilon_L^2 + \grave{o}_8 \upsilon_R{}^2) - \mu_{\chi_L}^2} \tag{15}$$

$$m_{\chi_R} = \sqrt{\frac{1}{2}(\grave{o}_7 \upsilon_L^2 + \grave{o}_9 \upsilon_R{}^2) - \mu_{\chi_R}^2} \tag{16}$$

$$m_{\rho} = \sqrt{\mu_{\rho}^2 + \frac{1}{2}(\grave{o}_{10} \upsilon_L^2 + \grave{o}_{11} \upsilon_R{}^2)} \tag{17}$$

$$m_{\omega} = \sqrt{\mu_{\omega}^2 + \frac{1}{2}(\grave{o}_{12} \upsilon_L^2 + \grave{o}_{13} \upsilon_R{}^2)} \tag{18}$$

The mass formulation of φ_L In Equation (11), the Higgs field mass in the Standard Model is the same as the Higgs field mass in the Standard Model. The Higgs field mass, according to experimental results, is 126 GeV. [31]. If the assumption is that $\upsilon_R > 30\upsilon_L$, then the mass of φ_L will be smaller than the mass of $\varphi_R; 30m_{\varphi_L} < m_{\varphi_R}$. If the VEV value υ_L =246 GeV and the Higgs scalar field mass m_{φ_L} = 126 GeV, the constant value λ_1 = 0.26 will get. The mass of the rest of the scalar field depends on the parameters. μ_i and $\grave{o}_i$. As in Equation 18, the scalar mass ω proportional to the mass term parameter μ_ω and the parameter ϵ_{12}, which indicates the interaction between scalars in the left sector ϕ_L and the parameter ϵ_{13}, which indicates the interaction between scalars in the right sector ϕ_R. Assuming the sequence of scalar field masses from the most massive to the lightest is $m_{\eta} > m_{\xi} > m_{\rho} > m_{\omega} > m_{\chi_L} > m_{\chi_R} > m_{\varphi_R} > m_{\varphi_L}$.

YUKAWA LAGRANGIAN

Interaction terms between the scalar field and fermions, which are invariant to gauge groups and violation of left-right symmetry, are generally shown by Equation (19). The symbol G shows the Yukawa coupling constant. The scalar field φ_L is defined as $\varphi_L = i\sigma_2 \varphi_L^*$. After spontaneous symmetry breaking, the scalar field acquires a VEV, and the fermions acquire mass via the Yukawa interaction after the scalar field develops a VEV. The scalar field is then expanded around its VEV. The Yukawa interaction can be written in the Lagrangian as:

$$\begin{aligned} L = {} & G_{\nu}(\overline{\ell_L}\varphi_L \nu_R + \overline{L_R}\varphi_R N_L) - G_e(\overline{\ell_L}\varphi_L e_R + \overline{L_R}\varphi_R E_L) \\ & -G_d(\overline{q_L}\varphi_L d_R + \overline{Q_R}\varphi_R D_L) - G_u(\overline{q_L}\widetilde{\varphi_L} u_R + \overline{Q_R}\widetilde{\varphi_R} U_L) - G_{e\eta}\overline{e_R}\eta\ E_L - G_{d\eta}\overline{d_R}\eta\ D_L - G_{u\eta}\overline{u_R}\eta\ U_L \\ & -G_{\nu N}\overline{\nu_R}\eta\ N_L - G_{ud}(\overline{u_R}\xi^* D_L + \overline{U_L}\xi^* d_R) - G_{\nu e}(\overline{\nu_R}\xi^* E_L + \overline{N_L}\xi^* e_R) - G_{\ell d}(\bar{\ell}\chi_L d_R + \overline{L_R}\chi_R^c D_L) \\ & -G_{qd}(\overline{Q_R}\chi_R D_L + \overline{q_L}\chi_L d_R) - G_{\ell u}(\overline{L_R}\widetilde{\chi_R} U_L + \overline{\ell_L}\widetilde{\chi_L} u_R) - G_{\nu q}(\overline{N_L}\widetilde{\chi_R} Q_R + \overline{\nu_R}\widetilde{\chi_L} q_L) \end{aligned}$$

$$-G_{\nu u}\left(\overline{\nu_R}\rho^* U_L + \overline{N_L}\rho^* u_R\right) - G_{ed}\left(\overline{e_R}\rho^* D_L + \overline{E_L}\rho^* d_R\right) - G_{eu}\left(\overline{e_R}\omega^* U_L + \overline{E_L}\omega^* u_R\right)$$
$$-G_{\nu d}\left(\overline{\nu_R}\omega^* D_L + \overline{N_L}\omega^* d_R\right) - G_{\nu\eta}\left(\overline{\nu_R}\eta\nu_R^C - \overline{N_L}\eta N_L^C\right)$$
$$-M_m\left(\overline{\nu_R}\nu_R^C + \overline{N_L}N_L^C\right) - M_d\overline{\nu_R}N_L + hc. \quad (19)$$

The fermion mass in this model is shown by the Equation (20)-(25).

$$m_e = \frac{G_e\upsilon_L}{\sqrt{2}}, \quad and \quad g(h_L\bar{e}e) = \frac{m_e}{\upsilon_L} \quad (20)$$
$$m_E = \frac{G_e\upsilon_R}{\sqrt{2}}, \quad and \quad g(h_R\bar{E}E) = \frac{m_E}{\upsilon_R} \quad (21)$$
$$m_d = \frac{G_d\upsilon_L}{\sqrt{2}}, \quad and \quad g\left(h_L\bar{d}d\right) = \frac{m_d}{\upsilon_L} \quad (22)$$
$$m_D = \frac{G_d\upsilon_R}{\sqrt{2}}, \quad and \quad g(h_R\bar{D}D) = \frac{m_D}{\upsilon_R} \quad (23)$$
$$m_u = \frac{G_u\upsilon_L}{\sqrt{2}}, \quad and \quad g(h_L uu) = \frac{m_u}{\upsilon_L} \quad (24)$$
$$m_U = \frac{G_U\upsilon_R}{\sqrt{2}}, \quad and \quad g(h_R\bar{U}U) = \frac{m_U}{\upsilon_R} \quad (25)$$

The electron mass formula and the up and down quark masses obtained from Equations (10), (22), and (23) have the same structure as the fermion mass mechanism in the Standard Model, namely originating from the Yukawa coupling connecting the left and right components after the electroweak symmetry breaking. [32]. Meanwhile, the mass in the right sector also has the same structure as the VEV value υ_R. The fermion mass presented in Equations (20)-(25) arises from the Yukawa interaction after the symmetry breaking, with its numerical value determined through experiments. Electron mass is precisely measured to be $m_e = 0.5109989461$ MeV, up-quark mass is $m_u = 2.16 \pm 0.07$MeV, and down-quark mass is $m_d = 4.70 \pm 0.07$ MeV. [33]. Neutrino mass generation does not like electron mass, down quarks, and up quarks in the left and right sectors. Instead, a neutrino mass is generated through the See-Saw Mechanism. The portion of Equation (19) that describes the neutrino is written in matrix form $\bar{\psi}A\psi$ with the basis $\psi = \left[\overline{\nu_L + \nu_L^C} \quad \overline{N_R + N_R^C} \quad \overline{\nu_R + \nu_R^C} \quad \overline{N_L + N_L^C}\right]$ and matrix A as shown by Equation (26).

$$A = \begin{bmatrix} 0 & 0 & -\frac{G_\nu\upsilon_L}{\sqrt{2}} & 0 \\ 0 & 0 & 0 & -\frac{G_\nu\upsilon_R}{\sqrt{2}} \\ -\frac{G_\nu\upsilon_L}{\sqrt{2}} & 0 & M_m & M_d \\ 0 & -\frac{G_\nu\upsilon_R}{\sqrt{2}} & M_d & M_m \end{bmatrix} \quad (26)$$

Matrix A in Equation (26) is a block matrix, $A = \begin{bmatrix} B & C \\ C & D \end{bmatrix}$. The A block matrix information in Equation (27).

$$B = \begin{bmatrix} 0 & 0 \\ 0 & 0 \end{bmatrix}; C = \begin{bmatrix} -\frac{G_\nu\upsilon_L}{\sqrt{2}} & 0 \\ 0 & -\frac{G_\nu\upsilon_R}{\sqrt{2}} \end{bmatrix}; D = \begin{bmatrix} M_m & M_d \\ M_d^T & M_m \end{bmatrix} \quad (27)$$

Assumed that the value of $M \gg \upsilon_R, \upsilon_L$, block matrix $D \gg C$, so the neutrino mass generation

process leads to the See-Saw Mechanism. In the LRS Model with an extra Scalar Field, the neutrinos are treated as Dirac neutrinos. The matrix A must be diagonalized to obtain the neutrino mass through the procedure $\bar{\psi} A\psi = \bar{\psi} UU^{\dagger} AUU^{\dagger}\psi = \left(\bar{\psi} U\right)\left(U^{\dagger} A\, U\right)\left(U^{\dagger}\psi\right)$. Diagonalized Matrix A is a matrix $U^{\dagger} AU$ with a diagonal matrix U and a new basis, namely $U^{\dagger}\psi$. In the see-saw mechanism, light neutrino masses, namely ν_L and N_R, and massive neutrino masses, namely ν_R and N_L, will be obtained.

EVOLUTION OF THE UNIVERSE TEMPERATURE

The temperature evolution scheme from post-inflation reheating to the occurrence of BBN is divided into three stages, as shown in Figure 1.

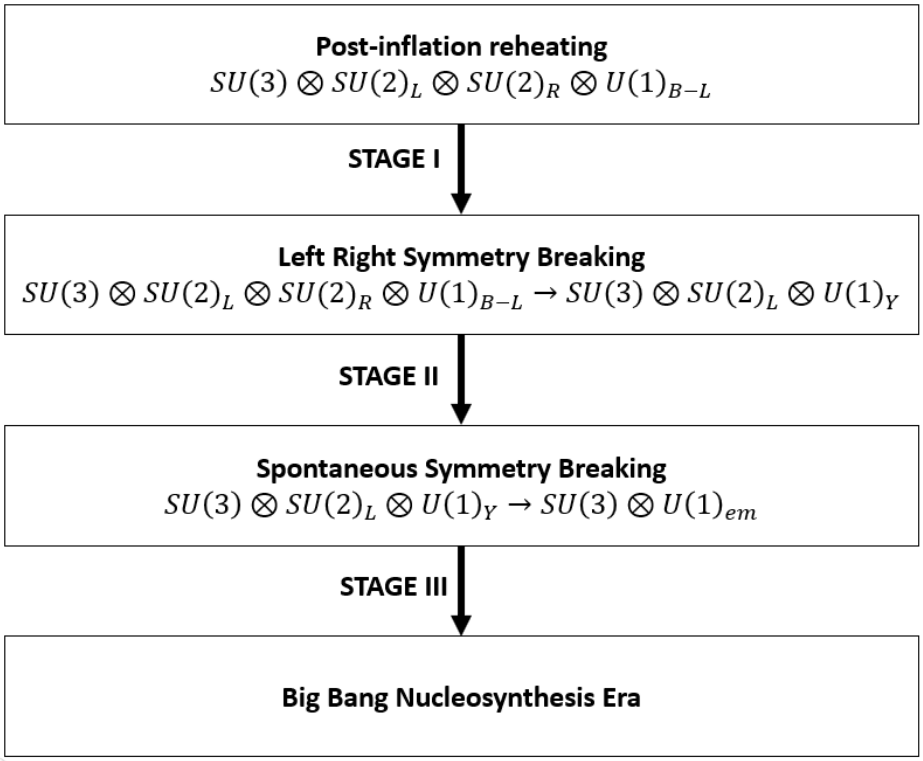

Figure 1. Schematic Flowchart of Temperature Evolution

Stage I. After Post-Inflation Reheating

After post-inflation reheating, the left sector gets additional heat from the decay of the massive particles ν_R and N_L in the left sector. The ratio of temperature in the left sector before the massive particles ν_R and N_L decay $\left(t_L \ll \tau_{\nu_R}\right)$ and after the massive particles ν_R and N_L decay $\left(t_L \gg \tau_{\nu_R}\right)$ into relativistic particles in the left sector in Equation (28).

$$\left(\frac{T_{fLI}}{T_{iLI}}\right)^4 \approx \frac{2,43 g_{*I}^{\frac{1}{3}}}{s_{\nu_R}^{\frac{4}{3}} m_{pl}^{\frac{2}{3}}}\left[\left(m_{\nu_R} n_{\nu_R}\right)^{\frac{4}{3}}\left(\sum_i \Gamma_{\nu_R}\right)_n^{-\frac{2}{3}} + \left(m_{N_L} n_{N_L}\right)^{\frac{4}{3}}\left(\sum_i \Gamma_{N_L}\right)_n^{-\frac{2}{3}}\right] \tag{28}$$

The symbol $\left(\sum_i \Gamma_{\nu_R}\right)_n^{-\frac{2}{3}}$ shows the total decay rate of neutrino υ_R, which decay into relativistic particles in the left sector. In contrast, $\left(\sum_i \Gamma_{N_L}\right)_n^{-\frac{2}{3}}$ is the total decay rate of neutrino N_L, which decay into relativistic particles in the left sector. A list of decay processes for massive particles ν_R and N_L which contribute entropy to the left sector along with their decay rates, can be seen in Table (2).

Table 2. Stage I: Entropy Contributor Interaction in the Left Sector

No	Decay Mode	Decay Rate	No	Decay Mode	Decay Rate
(a.1)	$\nu_R \to \widetilde{\phi_L} + \ell_L$	$\Gamma_{(a.1)} = \frac{G_\nu^2 m_{\nu_R}}{16\pi}$	(a.17)	$\overline{N_L} \to \overline{e_R} + \overline{u_R} + D_L$	$\Gamma_{(a.17)} = \frac{11}{96}\frac{G_{ud}^2 G_{ve}^2 m_N}{(4\pi)^3\hbar}$
(a.2)	$\nu_R \to \widetilde{\chi_L} + q_L$	$\Gamma_{(a.2)} = \frac{G_{\nu q}^2 m_{\nu_R}}{16\pi}$	(a.18)	$\overline{N_L} \to \overline{e_R} + \overline{U_L} + d_R$	$\Gamma_{(a.18)} = \frac{11}{96}\frac{G_{ve}^2 G_{ud}^2 m_{N_L}}{(4\pi)^3\hbar}$
(a.8)	$N_L \to \rho^* + u_R$	$\Gamma_{(a.8)} = \frac{G_{\nu u}^2 m_{N_L}}{16\pi}$	(a.23)	$\overline{N_L} \to \overline{u_R} + \overline{e_R} + D_L$	$\Gamma_{(a.23)} = \frac{11}{96}\frac{G_{\nu u}^2 G_{ed}^2 m_{N_L}}{(4\pi)^3\hbar}$
(a.9)	$N_L \to \omega^* + d_R$	$\Gamma_{(a.9)} = \frac{G_{\nu d}^2 m_{N_L}}{16\pi}$	(a.24)	$\overline{N_L} \to \overline{u_R} + \overline{E_L} + d_R$	$\Gamma_{(a.24)} = \frac{11}{96}\frac{G_{\nu u}^2 G_{ed}^2 m_{N_L}}{(4\pi)^3\hbar}$
(a.10)	$N_L \to \xi^* + e_R$	$\Gamma_{(a.10)} = \frac{G_{\nu e}^2 m_{N_L}}{16\pi}$	(a.30)	$\overline{N_L} \to \overline{d_R} + \overline{U_L} + d_R^C$	$\Gamma_{(a.30)} = \frac{11}{96}\frac{G_{\nu d}^2 G_{ud}^2 m_{N_L}}{(4\pi)^3\hbar}$
(a.11)	$\nu_R \to \ell_L + \overline{q_L} + u_R$	$\Gamma_{(a.11)} = \frac{11}{96}\frac{G_\nu^2 G_u^2 m_\nu}{(4\pi)^3\hbar}$	(a.32)	$\overline{N_L} \to \overline{d_R} + \overline{u_R} + D_L^C$	$\Gamma_{(a.32)} = \frac{11}{96}\frac{G_{\nu d}^2 G_{ud}^2 m_{N_L}}{(4\pi)^3\hbar}$

Examples of model interaction (a.11) and (a.12) depicted through a Feynman diagram can be seen in Figure 2.

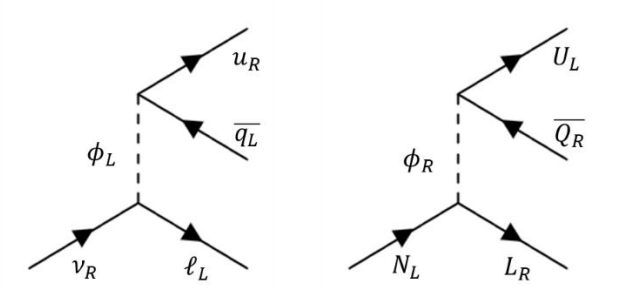

Figure 2. Feynman Diagram of Massive Neutrino Decay modes (a.11) and (a.12)

The massive neutrino decay interaction (a.11) is a decay process with the mediator φ_L producing three relativistic particles in the left sector. Modes (a.17) and (a.18) is a neutrino decay with the mediator ξ^*, which produces two left sector particles contributing entropy to the left sector and one right sector particle, namely D_L and $\overline{U}_L$ contributes entropy in the right sector. Assuming modes (a.17) and (a.18) only contribute entropy in the left sector. The neutrino ν_R is a non-relativistic massive particle $\left(m_{\nu_R} \gg T_{il}\right)$ whose particle density is the same for bosons and fermions, as shown by Equation (29).

$$n_{\nu_R} = g_{\nu_R}\left(\frac{m_{\nu_R}T_{iI}}{2\pi}\right)^{\frac{3}{2}}\exp\left[-\frac{m_{\nu_R}-\mu_{\nu_R}}{T_{iI}}\right] \tag{29}$$

The density of neutrino N_L also follows the same expression as ν_R particles. The entropy of the initial state when the neutrino particles ν_R and N_L just before decay is the entropy when the left sector temperature is equal to the neutrino mass $T_{iI} = m_{\nu_R}$ as shown by Equation (30).

$$s_{\nu_R} = \frac{2\pi^2}{45}g_{*I}T_{iI}^3 \tag{30}$$

The effective relativistic degrees of freedom in the left sector show the degrees of freedom of relativistic particles as shown by Equation (31).

$$g_{*I} = 3\cdot 2W_L + 2_B + 4_{\phi_L} + 2_\eta + 2_\xi + 4_{\chi_L} + 2_\rho + 2_\omega + 8^{(c)}\cdot 2_G + \frac{7}{8}\left(3\cdot 4_e + 3\cdot 2_\nu + 6\cdot 3^{(c)}\cdot 4_q\right) = 118.75 \tag{31}$$

The particles in the relativistic state in stage I are the $W_{L_{1,2,3}}$ field, the B field, which has two polarizations, the complex singlet scalar field η, ξ, ρ and ω with two intrinsic degrees of freedom, the complex doublet scalar field φ_L and χ_L has four intrinsic degrees; gluon has eight color combinations with two polarizations, electron-positron with three generations and two polarizations, ν_R neutrinos, and antineutrinos $\bar{\nu}_L$ with three generations and two polarizations, quarks-anti quarks three generations and every two polarizations.

In the right sector, the temperature ratio before the massive particles ν_R and N_L decay$\left(t_R \ll \tau_{N_L}\right)$ and after the massive particles ν_R dan N_L decay $\left(t_R \gg \tau_{N_L}\right)$ become relativistic particles in the left sector in Equation (32).

$$\left(\frac{T_{fRI}}{T_{iRI}}\right)^4 \approx \frac{2,43g_{*I}^{\frac{1}{3}\prime}}{s_{N_L}^{\frac{4}{3}}m_{pl}^{\frac{2}{3}}}\left[\left(m_{\nu_R}n_{\nu_R}\right)^{\frac{4}{3}}\left(\sum_i \Gamma_{\nu_R}\right)_n^{-\frac{2}{3}} + \left(m_{N_L}n_{N_L}\right)^{\frac{4}{3}}\left(\sum_i \Gamma_{N_L}\right)_n^{-\frac{2}{3}}\right] \tag{32}$$

The effective relativistic degrees of freedom in the right sector show the degrees of freedom of relativistic particles as shown by Equation (33).

$$g_{*I}^{'} = 3\cdot 2W_R + 2_B + 4_{\phi_R} + 2_\eta + 2_\xi + 4_{\chi_R} + 2_\rho + 2_\omega + 8^{(c)}\cdot 2_G + \frac{7}{8}\left(3\cdot 4_E + 3\cdot 2_N + 6\cdot 3^{(c)}\cdot 4_Q\right) = 118,75 \tag{33}$$

Suppose it is assumed that the temperature of the two sectors is the same, namely $T_{fL} = T_{fR_1}$, and the mass of the massive particles is $m_{\nu_R} = m_{N_L}$. In that case, the ratio between the two temperatures is equal to one, $T_{fL_1} = T_{fR_1}$. After post-inflation reheating, the temperature between the left sector is the same as the right sector term.

Stage II: Left-Right Symmetry Breaking

In stage II, after the left-right symmetry breaking occurs, the interaction is dominated by the decay process of the singlet scalar fields η, ξ, ρ and ω as well as the interaction process involving the doublet scalar fields χ_L and χ_R. The temperature change occurs when the temperature of the left sector is equal to the lifetime of the scalar field $\eta, t_L = \tau_\eta$. The scalar field η is assumed to be the most massive scalar field. The temperature ratio in the left sector before the scalar fields η, ξ, ρ, ω

and χ_L decay $\left(t_L \ll \tau_\eta\right)$ and after the scalar fields η,ξ,ρ,ω and χ_L decay $\left(t_L \gg \tau_\eta,\tau_\xi,\tau_\rho,\tau_\omega,\tau_{\chi L}\right)$ becomes a relativistic particle in the left sector shown by equation (34).

$$\left(\frac{T_{fLII}}{T_{iLII}}\right)^4 \approx \frac{2,43g_{*I\,I}^{\frac{1}{3}}}{s_\eta^{\frac{4}{3}}m_{pl}^{\frac{2}{3}}}[\left(m_\eta n_\eta\right)^{\frac{4}{3}}\left(\sum_i \Gamma_\eta\right)_n^{-\frac{2}{3}} + \left(m_\xi n_\xi\right)^{\frac{4}{3}}\left(\sum_i \Gamma_\xi\right)_n^{-\frac{2}{3}} + \left(m_\rho n_\rho\right)^{\frac{4}{3}}\left(\sum_i \Gamma_\rho\right)_n^{-\frac{2}{3}} + \left(m_\omega n_\omega\right)^{\frac{4}{3}}\left(\sum_i \Gamma_\omega\right)_n^{-\frac{2}{3}} + \left(m_{\chi_L} n_{\chi_L}\right)^{\frac{4}{3}}\left(\sum_i \Gamma_{\chi_L}\right)_n^{-\frac{2}{3}}] \tag{34}$$

The contributor to the entropy in the left sector during stage II is the scalar field scalar η,ξ,ρ,ω and χ_L decays. The scalar field η is assumed to be the most significant contributor to entropy because it is the most massive field. Entropy in stage II when the temperature of the left sector is equal to the mass of the scalar field $\eta, T_{i_{LII}} = m_\eta$. The amount of entropy is shown by Equation (35).

$$s_\eta = \frac{2\pi^2}{45} g_{*I\,I} T_{iII}^3 = \frac{2\pi^2}{45} m_\eta^3 g_{*II} \tag{35}$$

The density of the scalar field η with $g_\eta = 1, \mu_\eta = 0$ is shown by Equation (36).

$$n_\eta = g_\eta \left(\frac{m_\eta T_{iII}}{2\pi}\right)^{\frac{3}{2}} \exp\left[\mu_\eta - \frac{m_\eta}{T_{iII}}\right] = 0,36\frac{m_\eta^3}{\left(2\pi\right)^{\frac{3}{2}}} \tag{36}$$

The sum density of the scalar fields ξ,ρ,ω and χ_L follows the same formula as the sum density of the scalar field η in Equation (36). The relativistic degrees of freedom in the left sector after the left-right symmetry breaking occurs in stage II is 106.75. The scalar fields η,ξ,ρ,ω and χ_L are no longer relativistic because they have gained mass.

The right sector temperature change occurs when the right sector temperature is equal to the lifetime of the scalar field η, $t_R = \tau_\eta$. The scalar field η is assumed to be the most massive scalar field. The temperature ratio in the right sector before the scalar fields η,ξ,ρ,ω and χ_R decay $\left(t_R \ll \tau_\eta\right)$ and after the scalar fields η,ξ,ρ,ω and χ_R decay $\left(t_R \gg \tau_\eta,\tau_\xi,\tau_\rho,\tau_\omega,\tau_{\chi_R}\right)$ becomes a relativistic particle in the right sector shown by Equation (37). Symbol $\left(\sum_i \Gamma_\eta\right)_n^{-\frac{2}{3}}$ shows the total number of decay rates of the scalar field η, which decays into right sector relativistic particles, Symbol $\left(\sum_i \Gamma_\xi\right)_n^{-\frac{2}{3}}$ shows the number the total decay rate of the scalar field ξ which decays into relativistic particles in the right sector and so on.

$$\left(\frac{T_{fRII}}{T_{iRII}}\right)^4 \approx \frac{2,43g_{*I\,I}^{\frac{1}{3}\prime}}{s_\eta^{\frac{4}{3}}m_{pl}^{\frac{2}{3}}}[\left(m_\eta n_\eta\right)^{\frac{4}{3}}\left(\sum_i \Gamma_\eta\right)_n^{-\frac{2}{3}} + \left(m_\xi n_\xi\right)^{\frac{4}{3}}\left(\sum_i \Gamma_\xi\right)_n^{-\frac{2}{3}} + \left(m_\rho n_\rho\right)^{\frac{4}{3}}\left(\sum_i \Gamma_\rho\right)_n^{-\frac{2}{3}} + \left(m_\omega n_\omega\right)^{\frac{4}{3}}\left(\sum_i \Gamma_\omega\right)_n^{-\frac{2}{3}} + \left(m_{\chi_R} n_{\chi_R}\right)^{\frac{4}{3}}\left(\sum_i \Gamma_{\chi_R}\right)_n^{-\frac{2}{3}}] \tag{37}$$

The relativistic degree of freedom in the right sector is the same as the left sector, which is

106.75. There is a difference in relativistic degrees of freedom between the second and first stages because the scalar fields η, ξ, ρ, ω and χ_R, have acquired mass, so they are non-relativistic. The entropy and density of the scalar field η when the initial temperature of stage II in the right sector is equal to the mass of the scalar field η. The initial temperature of stage II in the left sector is the same as the final temperature of stage I in the left sector $T_{iL_{II}} = T_{fL_I}$ and the initial temperature of the right sector in stage II is the final temperature of the right sector of stage I, $T_{iR_{II}} = T_{fR_I}$.The temperature ratio between the right sector and the left sector of stage II is influenced by the mass of the scalar field χ_L and χ_R, and the final temperature ratio of stage II can be approximated as in Equation (38).

$$\left(\frac{T_{fR\,II}}{T_{fL\,II}}\right)^4 \approx \frac{m_{\chi_R}^2}{m_{\chi_L}^2} \tag{38}$$

The mass of the scalar field is $m_{\chi_R} < m_{\chi_L}$, so the left sector is hotter than the right sector.

Stage III: Spontaneous Symmetry Breaking

In stage III, the scalar fields φ_L and φ_R Get VEV values. The scalar field φ_L and the scalar field φ_R begin to decay into relativistic particles. The change in the left sector's temperature occurs when the left sector's temperature is equal to the lifetime of the scalar field. ϕ_L, $t_L = \tau_{\phi_L}$. The temperature ratio in the left sector before the φ_L scalar field decays $\left(t_L \ll \tau_{\phi_L}\right)$ and after the φ_L scalar field decays $\left(t_L \gg \tau_{\phi_L},\right)$ The relativistic particles in the left sector are shown by equation (39). The amount of entropy caused by the decay of the scalar field φ_L is shown by Equation (39).

$$\left(\frac{T_{fL\,III}}{T_{iL\,III}}\right)^4 \approx \frac{2,43 g_{*I\,I\,I}^{\frac{1}{3}}}{s_{\phi_L}^{\frac{4}{3}} m_{pl}^{\frac{2}{3}}} \left(m_{\phi_L} n_{\phi_L}\right)^{\frac{4}{3}} \left(\sum_i \Gamma_{\phi_L}\right)_n^{-\frac{2}{3}} \tag{39}$$

The amount of entropy caused by the decay of the scalar field φ_L is shown by Equation (40).

$$s_{\phi_L} = \frac{2\pi^2}{45} g_{*III} T_{iIII}^3 = \frac{2\pi^2}{45} m_{\phi_L}^3 g_{*III} \tag{40}$$

The density of the scalar field φ_L at the time of stage III when the initial temperature of stage II in the left sector is equal to the mass of the scalar field φ_L, $T_{iLIII} = m_{\phi_L}$ and with $g_{\phi_L} = 1, \mu_{\phi_L} = 0$ is $0,36(2\pi)^{-\frac{3}{2}} m_{\phi_L}^3$. The relativistic degrees of freedom in the left sector in this stage is 102.75 because the scalar field φ_L is no longer relativistic because it has gained mass.

In the right sector, the additional entropy in stage III contributes to the decay process of the ϕ_R scalar field into relativistic fermion particles. The right sector temperature change occurs when the right sector temperature is equal to the lifetime of the scalar field. $\varphi_R, t_R = \tau_{\phi_R}$. The temperature ratio in the right sector before $\left(t_R \ll \tau_{\phi_R}\right)$ and after $\left(t_R \gg \tau_{\phi_R},\right)$the scalar field φ_R decays to relativistic particles in the right sector is shown by equation (41).

$$\left(\frac{T_{fR\,III}}{T_{iR\,III}}\right)^4 \approx \frac{2,43 g_{*R\,I\,I\,I}^{\frac{1}{3}}}{s_{\phi_R}^{\frac{4}{3}} m_{pl}^{\frac{2}{3}}} \left(m_{\phi_R} n_{\phi_R}\right)^{\frac{4}{3}} \left(\sum_i \Gamma_{\phi_R}\right)_n^{-\frac{2}{3}} \tag{41}$$

As in the left sector, a consistent pattern is observed across both sectors. The final temperature ratio from stage I to stage III between the right sector and the left sector is shown by Equation (42).

$$\left(\frac{T_{fRIII}}{T_{fLIII}}\right)^4 \approx \frac{m_{\phi_R}^{\frac{2}{3}} m_{\chi_R}^2}{m_{\phi_L}^{\frac{2}{3}} m_{\chi_L}^2} \tag{42}$$

Based on Equation (45), the masses influence the temperature ratio between the right sector and the left sector. $m_{\phi_L}, m_{\chi_L}, m_{\phi_R}$ and m_{χ_R}. With the same assumption in the final stage II, the temperature of the left sector is higher than the right sector in the final stage III.

BIG BANG NUCLEOSYNTHESIS IN THE LEFT-RIGHT SYMMETRY MODEL WITH AN EXTRA SCALAR FIELD

The left and right sectors must have had different temperatures when BBN occurred. This prevents the mirror sector from coming into thermal contact with the standard sector. If both sectors were in the same thermal equilibrium, it would produce an effective neutrino number N that exceeds the limit allowed by the BBN constraints. The right sector temperature must be lower than the left when BBN occurs, according to research results. [12,34]. For the temperature ratio between sectors to comply with BBN constraints, it is necessary to know the lower limit of the scalar field mass ratio. ϕ_R, χ_L and χ_R. Based on the observation results, the additional new relativistic particles that are allowed according to BBN predictions are $\Delta N < 0.2 - 0.3$, so for $\Delta N < 0.2 - 0.3$, the additional relativistic degrees of freedom are $\Delta g_* < 0.4 - 0.5$.

The particles in the right sector that remain relativistic are the light neutrinos. N_R. As a result, these particles introduce a new contribution to the relativistic degrees of freedom during the BBN era. The connection between the relativistic degrees of freedom and the temperature ratio of the right and left sectors is $\left(T_{fR}/T_{fL}\right)_{BBN}^4 < 0,08 - 0,09$. The scalar field φ_L, identified as a Standard Model Higgs particle, has a well-established mass of 126 GeV[31]. According to Equation (15), the mass of φ_R is proportional to υ_R, while $\upsilon_R > 30\upsilon_L$ [29]. Thus, the mass of φ_R can be estimated as $m_{\phi_R} \approx 30$. If we put it into equation (42), we get the ratio. $m_{\chi_R}/m_{\chi_L} \approx 0,09 - 0.10$. This mass ratio between the right and the left sector scalar fields shows that the mass of χ_R is more massive than the mass of χ_R, $m_{\chi L} > m_{\chi_R}$.

The left sector temperature exceeds the right sector temperature. This indicates that Big Bang Nucleosynthesis in the right sector took place earlier than in the left sector. In the left sector, BBN occurs when the temperature decreases by about 1 MeV, and the n-p mass difference of around 1.3 MeV causes the number of protons to be greater than that of neutrons. The decay rate of neutrons into protons is lower than the Universe's expansion rate. When this happens, the decay of neutrons into protons occurs less frequently so that the ratio between neutrons and protons remains constant. The temperature at which this happens is called $T_{freeze\ out} \sim 0,75$ MeV. [3]. The result is that about 25% of the baryons are converted into primordial Helium-4, 75% into hydrogen, and small amounts of other light elements. By maintaining the right sector's temperature lower than the left sector's temperature during BBN, this model ensures that the contribution of baryons from the right industry to the primordial Helium-4 abundance remains consistent with the predictions of standard BBN, avoiding any significant deviations. This means that despite the contribution from light neutrinos in the right sector, the level of additional relativistic particles is still within the limits

allowed by BBN.

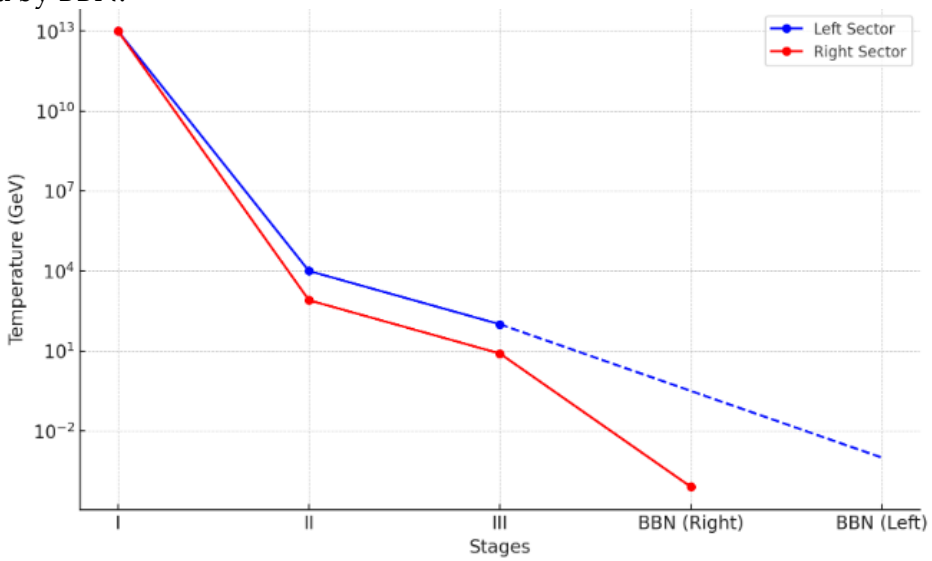

Figure 3. Temperature evolution until BBN occurs in the Left-Right sectors

Big Bang Nucleosynthesis (BBN) in the right sector is qualitatively similar to the left sector, but it occurred earlier, as shown in Figure 3. The expansion rate is greater than the neutron-proton decay rate, so the right sector Neutron-Proton ratio is constant at higher temperatures $T_{R_{freezeout}} > T_{L_{freezeout}}$. Therefore, right-sector neutrons have shorter decay times. The ratio between Neutron-proton right is proportional to one. In the right sector, neutrons are produced and removed by weak interactions via the reaction in Equation (43).

$$n' + \bar{E} \rightarrow p' + \bar{N}, \qquad p' + E \rightarrow n' + N \tag{43}$$

The decay of the right sector neutron $n' \rightarrow p' + E + \bar{N}$ can be neglected because the BBN takes place in the first 10 seconds or so, this time is shorter than the lifetime of the right sector neutron $\tau_n \sim 886s$. The approximate formula for the mass fraction of Helium-4 in the right sector in the reference is shown by Equation (5). [27,28]. The symbol $t_N \sim 200s$ shows the age of the universe at the time of deuterium freeze-out. Symbol $T_W \sim 0.75$ MeV is magic when $n' \leftrightarrow p'$ freezeout. Thus, the primordial Helium-4 abundance is obtained in the right sector as shown by Equation (44).

$$Y_{4R} \cong 79\% - 87\% \tag{44}$$

The primordial Helium-4 abundance in the right sector is higher than in the left sector $Y_{4R} > Y_{4L}$. This is consistent with research by Berezhiani et al. [27] and Roux and Celine [28]. Notably, the primordial Helium-4 abundance in the right sector has no impact on the abundance in the left sector. Given its abundance, primordial Helium-4 in the right industry emerges as a potential candidate for dark matter.

CONCLUSION

The Left-Right Symmetry Model with an additional scalar field ensures that baryon contributions to primordial Helium-4 from the right sector do not disrupt standard BBN predictions by keeping a lower temperature in the right sector during BBN. The temperature ratio between the right and left sectors during Big Bang Nucleosynthesis (BBN) is. The rresponding BBN constrainis $m_{\chi_R}/m_{\chi_L} \approx 0{,}09 - 0.10$. According to the Standard Model, the abundance of primordial

Helium-4 in the left sector remains 25% due to Big Bang Nucleosynthesis (BBN) constraints. In contrast, the earlier onset of BBN in the right sector leads to a more efficient production of light nuclei, resulting in a significantly larger primordial Helium-4 abundance of approximately 79%-87%.

The helium-4 abundance in the right sector does not affect the helium abundance in the left sector. Furthermore, the higher helium-4 abundance compared to the left sector ensures compatibility with the Big Bang Nuclear Force (BBN) constraint. This higher abundance of helium-4 could be a candidate for dark matter; therefore, it needs further research.

REFERENCES

[1] E. W. Kolb and M. S. Turner, *The Early Universe*. New york: Addison-Wesley Publishing Company, 1990. Doi.

[2] S. Sarkar, "Big bang nucleosynthesis and physics beyond the standard model," *Reports Prog. Phys.*, vol. 59, no. 12, pp. 1493–1609, 1996. Doi. https://doi.org/10.1088/0034-4885/59/12/001

[3] V. A. Rubakov and S. Gorbunov, D., *Introduction to The Theory Of The Early Universe Hot Big Bang Theory*. World Scientific, 2011. Doi. https://doi.org/10.1142/7874

[4] V. Berezinsky, M. Narayan, and F. Vissani, "Mirror model for sterile neutrinos," *Nucl. Phys. B*, vol. 658, no. 1–2, pp. 254–280, 2003. Doi. https://doi.org/10.1016/S0550-3213(03)00191-3

[5] B. C. Allanach, "Beyond the standard model," *Cern Yellow Reports Sch. Proc.*, vol. 5, no. June, pp. 123–152, 2017. Doi. https://doi.org/10.23730/CYRSP-2017-005.123

[6] K. Abe *et al.*, "Constraint on the matter–antimatter symmetry-violating phase in neutrino oscillations," *Nature*, vol. 580, no. 7803, pp. 339–344, 2020. Doi. https://doi.org/10.1038/s41586-020-2177-0

[7] D. O'Connell, M. J. Ramsey-Musolf, and M. B. Wise, "Minimal extension of the standard model scalar sector," *Phys. Rev. D - Part. Fields, Gravit. Cosmol.*, vol. 75, no. 3, pp. 1–4, 2007.

[8] S. R. Haniah, Istikomah, M. A. Khalif, and H. H. Kusuma, "Scalar Field Mass Generation in the Gauge Theory SU(2)XU(1)XZ2," in *Journal of Physics: Conference Series*, 2020. Doi. https://doi.org/10.1088/1742-6596/1539/1/012005

[9] B. Dutta, Y. Mimura, and R. N. Mohapatra, "An SO(10) grand unified theory of flavor," *J. High Energy Phys.*, vol. 34, 2010. Doi.

[10] F. J. de Anda, S. F. King, and E. Perdomo, " S U (5) grand unified theory with A 4 modular symmetry ," *Phys. Rev. D*, vol. 101, no. 1, p. 15028, 2020. Doi. https://doi.org/10.1103/PhysRevD.101.015028

[11] R. N. Mohapatra and S. Nasri, "Avoiding BBN constraints on mirror models for sterile neutrinos," *Phys. Rev. D - Part. Fields, Gravit. Cosmol.*, vol. 71, no. 5, pp. 1–7, 2005. Doi. https://doi.org/10.1103/PhysRevD.71.053001

[12] M. Satriawan, "A Multicomponent Dark Matter in a Model with Mirror Symmetry with Additional Charged Scalars," no. 1, pp. 1–9, 2018. Doi. https://doi.org/10.48550/arXiv.1801.00326

[13] M. Kawasaki, K. Kohri, T. Moroi, and Y. Takaesu, "Revisiting big-bang nucleosynthesis constraints on long-lived decaying particles," *Phys. Rev. D*, vol. 97, no. 2, p. 23502, 2018. Doi. https://doi.org/10.1103/PhysRevD.97.023502

[14] A. Boyarsky, M. Ovchynnikov, O. Ruchayskiy, and V. Syvolap, "Improved big bang nucleosynthesis constraints on heavy neutral leptons," *Phys. Rev. D*, vol. 104, no. 2, p. 23517,

2021. Doi. https://doi.org/10.1103/PhysRevD.104.023517

[15] J. C. Pati and A. Salam, "Lepton Number As The Fourth 'color,'" *Phys. Rev. D*, vol. 10, 1974.

[16] E. Akhmedov, M. Lindner, E. Schnapka, and J. W. F. Valle, "Dynamical Left-Right Symmetry Breaking," no. September, 1995. Doi. https://doi.org/10.1103/PhysRevD.53.2752

[17] A. Damanik, M. Satriawan, and P. Anggraita, "Left-Right Symmetry Model with Two Bidoublets and One Doublet Higgs Fields for Electroweak Interaction." https://www.academia.edu/15378835/Left_Right_Symmetry_Model_with_Two_Bidoublets_and_One_Doublet_Higgs_Field_for_Electroweak_Interaction

[18] R. N. Mohapatra and G. Senjanovic, "Exact Left-Right Symmetry and Spontaneous Violation o Parity," *Phys. Rev. D*, vol. 10, 1975. Doi. https://doi.org/10.1103/PhysRevD.12.1502

[19] S. Patra, "Neutrinoless double beta decay process in left-right symmetric models without scalar bidoublet," *Phys. Rev. D - Part. Fields, Gravit. Cosmol.*, vol. 87, no. 1, 2013. Doi. https://doi.org/10.1103/PhysRevD.87.015002

[20] Istikomah, "Pembangkitan Massa Medan Skalar dan Boson Tera pada Model Simetri Kiri Kanan Termodifikasi Berdasarkan Grup Tera SU(3)⊗SU(2)_L⊗SU(2)_R⊗U(1)_Y," *J. Fis.*, vol. 10, no. 2, pp. 35–41, 2020. Doi. https://doi.org/10.21580/jnsmr.2023.9.1.17481

[21] A. S. Adam, A. Ferdiyan, and M. Satriawan, "A New Left-Right Symmetry Model," *Adv. High Energy Phys.*, vol. 1, 2020. Doi. **https://doi.org/10.1155/2020/3090783**

[22] A. Ferdiyan, A. S. Adam, and M. Satriawan, "The Left-Right Symmetry Breaking Mechanism for the New Left-Right Symmetry Model," *JPSE (Journal Phys. Sci. Eng.*, vol. 5, no. 1, pp. 1–5, 2020. Doi. https://doi.org/10.28932/jpse.v5i1.12882

[23] N. E. Isnawati, I. Istikomah, and M. A. Khalif, "Fermion mass formulation in the Modified Left-Right Symmetry Model," *J. Nat. Sci. Math. Res.*, vol. 8, no. 2, pp. 66–74, 2022. Doi. https://doi.org/10.21580/jnsmr.2022.8.2.13633

[24] Istikomah and N. E. Isnawati, "Scalar fields as dark matter candidates in the modified left-right symmetry model," vol. 9, no. 1, pp. 19–28, 2023. Doi. https://doi.org/10.21580/jnsmr.2023.9.1.17481

[25] D. Griffiths, *Introduction to Elemntary Particles*, Second, Re. WILEY-VCH Verlag GmbH & Co. KGaA, 2008.

[26] Istikomah, "Kendala Big Bang Nucleosynthesis Pada model Cermin Termodifikasi," Universitas Gadjah Mada, 2015.

[27] Z. Berezhiani, D. Comelli, and F. L. Villante, "The early mirror universe: Inflation, baryogenesis, nucleosynthesis and dark matter," *Phys. Lett. Sect. B Nucl. Elem. Part. High-Energy Phys.*, vol. 503, no. 3–4, pp. 362–375, 2001. Doi. https://doi.org/10.1016/S0370-2693%2801%2900217-9

[28] J. S. Roux and J. M. Cline, "Constraining galactic structures of mirror dark matter," *Phys. Rev. D*, vol. 102, no. 6, 2020. Doi. https://doi.org/10.1103/PhysRevD.102.063518

[29] Y. A. Coutinho, J. A. Martins Simões, and C. M. Porto, "Fermion masses in a model for spontaneous parity breaking," *Eur. Phys. J. C*, vol. 18, 2001. Doi. https://doi.org/10.1007/s100520100525

[30] P. D. B. Collins, A. D. Martin, and E. J. Squaires, *Particle Physics and Cosmology*. John Willey & Sons, 1989.

[31] The ATLAS Collaborations, "Observation of a new particle in the search for the Standard Model Higgs boson with the ATLAS detector at the LHC," vol. 716, no. May, pp. 1–29, 2013.

Doi. https://doi.org/10.1016/j.physletb.2012.08.020
[32] F. Halzen and A. D. Martin, *Quark And Leptons: an Introductory Course in Modern Particle Physics*. John Willey & Sons, 1984.
[33] S. Navas *et al.*, "Review of particle physics," *Phys. Rev. D*, vol. 110, no. 3, 2024.
[34] R. Foot, "Mirror dark matter: Cosmology, galaxy structure and direct," *Int. J. Mod. Phys. A*, vol. 29, no. 11–12, 2014. Doi. https://doi.org/10.1142/S0217751X14300130